

Efficient Moment Frame Structure

Mircea I. Pastrav, Cornelia Baera, Florea Dinu

Abstract—A different concept for designing and detailing of reinforced concrete precast frame structures is analyzed in this paper. The new detailing of the joints derives from the special hybrid moment frame joints. The special reinforcements of this alternative detailing, named modified special hybrid joint, are bondless with respect to both column and beams. Full scale tests were performed on a plan model, which represents a part of 5 story structure, cropped in the middle of the beams and columns spans. Theoretical approach was developed, based on testing results on twice repaired model, subjected to lateral seismic type loading. Discussion regarding the modified special hybrid joint behavior and further on widening research needed concludes the presentation.

Keywords—Acceptance criteria, modified hybrid joint, repair, seismic loading type.

I. INTRODUCTION

AN experimental study concerning a different concept for designing and detailing of reinforced concrete precast frame structures has been developed starting with 2009, in Cluj-Napoca URBAN INCERC test laboratory.

The theoretical approach is based on another design concept for the seismic loading assessment using Direct Displacement-Based Design method [1] and on a different type of frame joints detailing.

The new detailing of the moment resistant joints derives from the special hybrid moment frame joints which are designed with respect to the provision given by [2]. The precast RC structure is assembled by non-adherent post-tensioned tendons. The joints are called hybrid due to the fact they contain both prestressed and mild reinforcement. The tendons must be designed to remain elastic up to the failure of special reinforcement, so they are tensioned at a lower level compare to the usual prestressed building elements. This allows them to develop considerable large elastic elongation when the structure has to withstand accidental loadings and then, after the loading action stops, to release the stored energy and to induce the structure self-balance.

The essential characteristic of the special hybrid moment frame joint consists in the special reinforcement connection detailing of the precast members. The hybrid joint has the special reinforcement debonded on two limited zones at the interface of column-beam joint, where yielding is expected to

occur under seismic loadings. The special reinforcements of this alternative detailing, named modified special hybrid joint, are bondless with respect to both column and beams, and are fixed only at their ends, thus acting as tension rods [3] and [4].

The modified hybrid joints have almost the same structural behavior as classical hybrid joints. Moreover, the modified hybrid joints detailing allows the replacement of the special ductile reinforcement, when damaged by a strong earthquake or other high magnitude accidental loading [5]. This characteristic is detailed further on, based on the results of a number of three tests performed on a modified hybrid joint model.

The behavior of repaired specimen representing a modified special hybrid moment frame joint subjected to seismic type loadings is analyzed further on.

II. EXPERIMENTAL PROGRAM

A. Test Model

The tests were performed on a full scale plan model, which represents a part of 5 story structure, cropped in the middle of the beams and columns spans. A detailed presentation of the design of the actual structure is given in [3] and [4].

A brief description of the model detailing is necessary in order to facilitate the understanding of its behavior under loadings.

As the members have to respect the provisions of ordinary frame elements, the joint detailing are different designed. The ends of the beams must contain at both upper and lower ducts corresponding to column engulfed ones, where ductile steel bars are introduced. This reinforcement, named special, is symmetrically disposed with respect to the centroid of the beams and it has several roles in the joint resistant mechanism. The most important one is to assure yielding type energy dissipation.

Due to the fact that special reinforcement is only connected to the beam ends, it can be removed in case of large elongation or failure and be simply replaced by a new one.

Considering this important characteristic, a single model has been manufactured, and it has been several times tested. The experimental program was focused on its behavior under lateral cyclic loading and also on its reparability capabilities.

The procedure improves data gathering using the same amount of resources as in common cases.

The specimen has been tested to seismic type lateral loadings, using the given displacement and resultant force test procedure.

During the tests there were carefully monitored and registered the main behavior aspects as: lateral displacements, related lateral force, cracking pattern, joint openings “cracks”, special reinforcement behavior have been monitored and

M. I. Pastrav is with the National Institute for Research and Development in Construction, Urban Planning and Sustainable Spatial Development “URBAN-INCERC”, Cluj-Napoca Branch, Romania, (phone: +40264 425 462; fax: +40264 425 988; e-mail: mircea.pastrav@incerc-cluj.ro).

C. Baera is with the National Institute for Research and Development in Construction, Urban Planning and Sustainable Spatial Development “URBAN-INCERC”, Cluj-Napoca Branch, Romania, (e-mail: cornelia.baera@incerc-cluj.ro).

F. Dinu is with “Politehnica” University Timisoara, Romania, (e-mail: florea.dinu@upt.ro).

registered. Based on these data hysteretic loops lateral force vs. top displacement has been drawn and dissipated energy has

been determined. The specimen and also static scheme of the tests is sketched in Fig. 1.

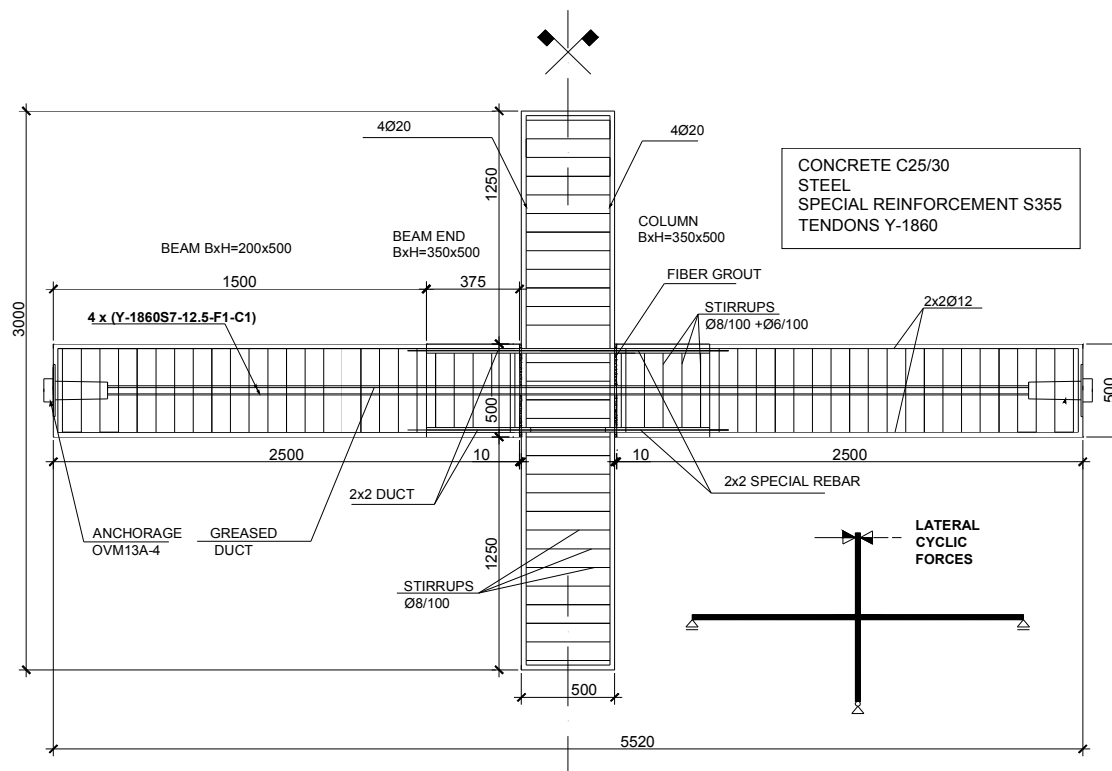


Fig. 1 Test specimen and static scheme

The mean value of cubic compressive strength of the concrete kept in the same conditions as the specimen, determined at age of 28 days, is 34MPa.

The repairs consisted in replacement of the special reinforcements damaged during testing.

For the first repair 12 mm diameter treaded rods, 4.8 group, were used, as presented in Fig. 2.

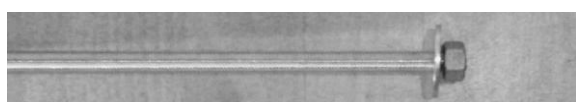


Fig. 2 Special reinforcement for the first repair of the model N2c

The actual mechanical properties of the treaded rods are given in Table I.

Yielding stress, R_{el} [MPa]	Ultimate tensile strength, R_m [MPa]	Remanent elongation after failure, A_5 [%]
346	489	15.5

For the second repair 12 mm diameter B500B steel rods were used.

The treaded ends were specially manufactured so that the minimum diameter in the connection length to be greater than

the current one, in order to avoid failure in the connection zones, as can be seen in Fig. 3.



Fig. 3 Special reinforcement for the second repair of the model N2d

The actual mechanical properties are given in Table II.

Yielding stress, R_{el} [MPa]	Ultimate tensile strength, R_m [MPa]	Remanent elongation after failure, A_5 [%]
513	602	16.6

B. Load History

The model has been 3 times tested according to the diagram in Fig. 4.

The initial test was carried out up to a story drift ratio equal to 0.025, with respect to the actual structure, according to [6].

The other two tests were performed up to a story drift ratio equal to 0.035, with 3 complete cycles at a certain imposed displacement, followed by a monotonous loading up to the failure of the special reinforcement. The load history is actually a displacement one.

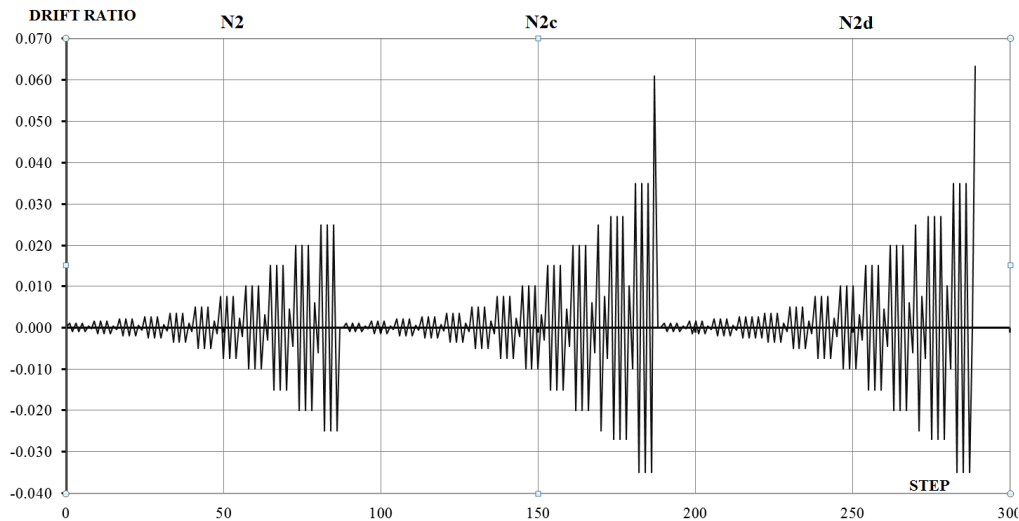


Fig. 4 Displacement history

C. Experimental Results

Aspects during the testing are shown in Fig. 5 for the first time repaired model N2c, respectively in Fig. 6 for the second time repaired model N2d.



Fig. 5 Second test of the model – N2c

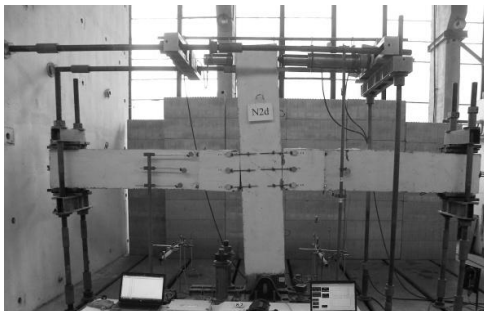


Fig. 6 Third test of the model – N2d

Opposite to the classical RC frame joint detailing, where the deformations develop in the whole structure, when hybrid joints are used, the horizontal elements have practically rigid body displacements.

The most of the beams deformations occur due to the opening and closing of cracks located at the column-beam

interface. As a consequence the critical damages are located only in the vicinity of joint areas.

The main results for the repaired model tests are better highlighted by the lateral loading vs. top column displacements.

The hysteretic diagrams are presented in Fig. 7 for the first time repaired model N2c.

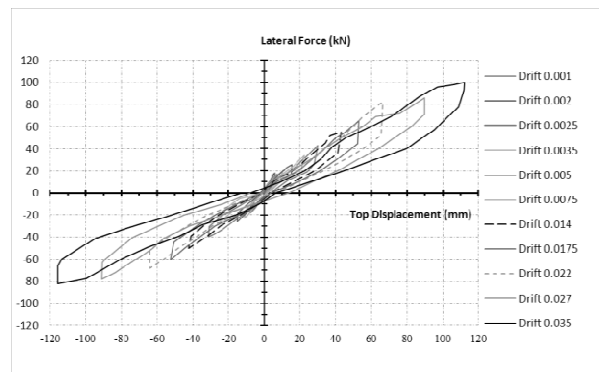


Fig. 7 Envelope diagrams for N2c test

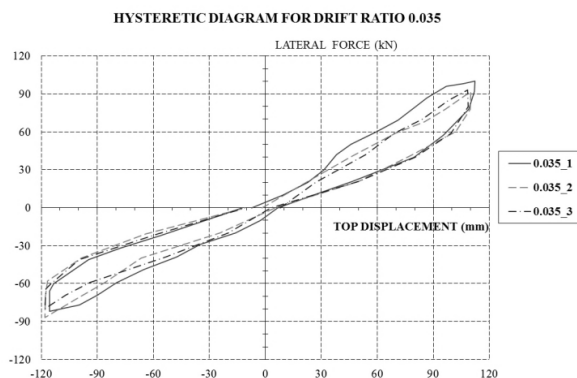


Fig. 8 Maximum drift ratio diagrams for N2c test

In Fig. 8 is presented the hysteresis diagram for the 0.035 drift ratio for the first time repaired model N2c.

The hysteretic diagrams are presented in Fig. 9 for the second time repaired model N2d.

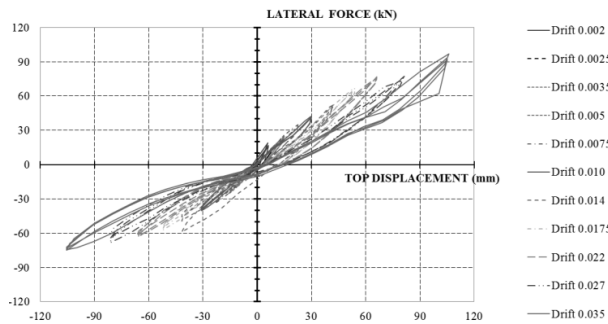


Fig. 9 Hysteretic diagrams for N2d test

The modified hybrid joint model proves a self-balancing behavior after the external loadings removal, due to the post-tensioned non-adherent tendons, as shown in Fig. 10 for the first time repaired model N2c.

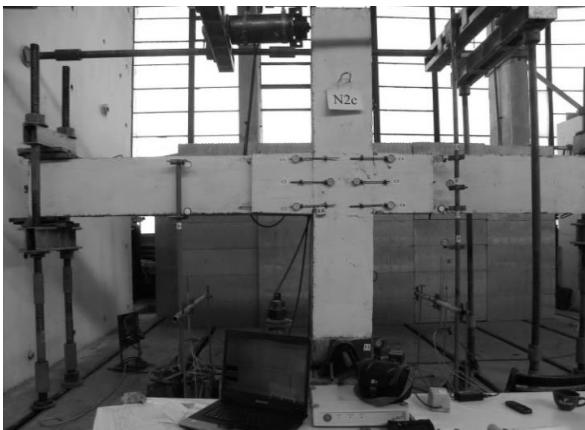


Fig. 10 Model N2c after the test



Fig. 11 Detail of N2d after test

The cracks at the interfaces beam-column are virtually

closed after the loading removal.

After the third test, the model N2d was seriously damaged as can be seen in Fig. 11.

The dissipated energy through elastic friction, hysteresis phenomenon and post-elastic deformation, at the first cycle of each lateral displacement magnitude is presented in Fig. 12.

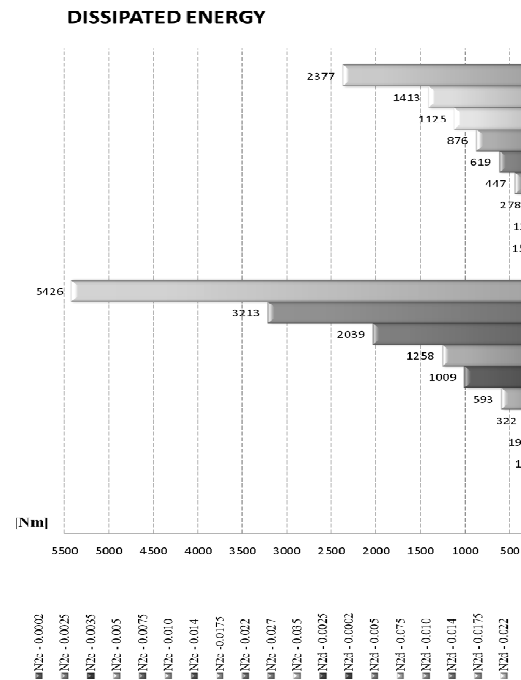


Fig. 12 Dissipated energy

III. THEORETICAL APPROACH

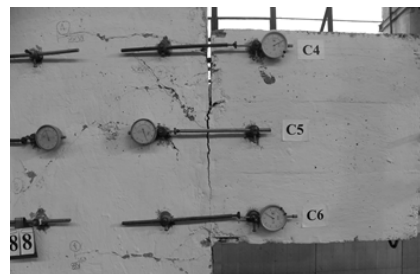


Fig. 13 Actual rotation at column-beam interface before special reinforcement failure

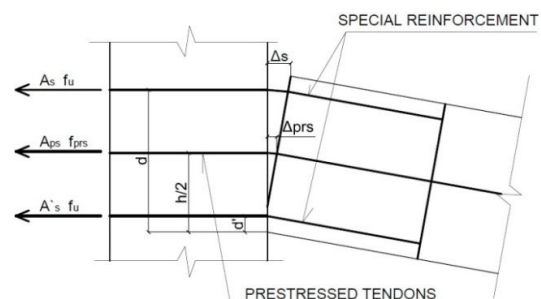


Fig. 14 Rotation at column-beam interface

A new set of equations for the estimation of probable flexural strength of modified hybrid joint is proposed, based on actual recorded rotation at the column-beam interface, as can be seen in Fig. 13.

The theoretical mechanism is presented in Fig. 14.

The special rebar elongation (Δ_s) at the column-beam interface is calculated as a sum of elastic and post elastic strains:

$$\Delta_s = \varepsilon_y \cdot l + l_d \cdot A_n \quad (1)$$

where:

ε_y - elastic strain limit (yielding strain) of the special rebars;

l - special rebar length;

l_d - development length of plastic strain;

A_n - minimum remanent elongation after failure.

The elongation of the tendons (Δ_{prso}), due to one joint interface opening, is estimated by the equation:

$$\Delta_{prso}/\Delta_s = (h/2-c)/(d-c) \quad (2)$$

where:

h - beam depth;

d - distance from extreme compression fiber of the grout pad at interface to the opposite side special reinforcement centroid;

c - distance from extreme compression fiber of grout pad to neutral axis at beam-column interface.

The position of the neutral axis is estimated considering the inner forces equilibrium, considering that both special reinforcements are in tension:

$$f_c \cdot b \cdot c = f_u \cdot (A_s + A'_s) + A_{ps} \cdot f_{prs} \quad (3)$$

where:

f_c - concrete strength for accidental loading ($f_{ck}/1.2$);

b - width of the beam-column interface

f_u - ultimate strength of special reinforcement;

A_s - area of special reinforcement placed opposite to compression zone of the grout pad at the column-beam interface;

A'_s - area of special reinforcement in compression zone of the grout pad at the column-beam interface;

A_{ps} - area of prestressed reinforcement;

f_{prs} - stress in prestressed reinforcement;

$$f_{prs} = f_{se} + \Delta\sigma_{prso} \quad (4)$$

where:

f_{se} -effective stress in post-tensioning tendons, after allowance of all losses;

$\Delta\sigma_{prso}$ - tension stress increase in strands due to the opening of the cracks at the interfaces.

The tension stress increase is considered as a consequence of all interfaces elongations. The tension growth in tendons is given by the equation:

$$\Delta\sigma_{prso} = n \cdot \Delta_{prso} \cdot E_p / L \quad (5)$$

where:

n - number of beam-column interfaces;

L - tendons length between anchorages;

E_p - elasticity modulus of prestressed tendons.

The probable flexural strength at the beam-column interfaces is estimated as the sum of the contribution of special bars and also of the prestressed tendons:

$$M_{pr} = A_{ps} \cdot f_{prs} (h-c)/2 + A_s \cdot f_u (d-c)/2 \quad (6)$$

The estimated values calculated using the proposed relationships (1)–(6) and nominal and effective material properties are presented in Table III.

TABLE III
ASSESSED LATERAL RESISTANCE

Special rebar type	$E_n (M_n) [kNm]$	$E_{pr} (M_{pr}) [kNm]$
Threaded rods	132.9	139.7
B500B	142.8	153.5

IV. PERFORMANCE OF THE MODEL UNDER SEISMIC TYPE LOADING

The behavior of the repaired model at both tests is evaluated according to the acceptance criteria [7], which can be briefly expressed by the following equations:

$$E_{max} > E_n \quad (7)$$

$$E_{max} < \lambda \cdot E_n \quad (8)$$

$$F_{max3} > 0.75 \cdot F_{max1} \quad (9)$$

$$\beta > 0.125 \quad (10)$$

$$K_{s(\theta=0.035)} > 0.05 \cdot K_{s(\theta=0.001)} \quad (11)$$

where:

E_{max} - maximum lateral resistance of test module, determined from test results (forces or moments);

E_n - nominal lateral resistance of test module, determined using specified geometric properties of test members, specified yield strength of reinforcement, specified compressive strength of concrete; strength reduction factor ϕ of 1.0;

E_{pr} - probable lateral resistance of test module determined using actual geometric and material properties of test members; strength reduction factor ϕ of 1.0;

λ - column over strength factor used for test module;

θ - drift ratio;

F_{max} - maxim lateral loading,

n - number of loading cycle at the same displacement;

β - relative energy dissipation ratio, which can be defined as ratio of actual to ideal energy dissipated by test module during reversed cyclic response between given drift ratio limits, expressed as the ratio of the area of the hysteresis loop for that cycle to the area of the circumscribing parallelograms defined

by the initial stiffness during the first cycle and the peak resistance during the cycle for which the relative energy dissipation ratio is calculated;

K_s – dissipated energy;

Tables IV and V present the evaluation of the behavior of the first time repaired model, N2c, and respectively of the second time repaired model, N2d, by the means of the up-mentioned acceptance criteria (7)–(11).

TABLE IV
MODEL N2C

Criterion	Values	Conclusions
$E_{max} > E_n$	$M_{max} = 141 \text{ KNm}$ $M_n = 132.9 \text{ KNm}$	OK
$E_{max} < \lambda E_n$	$M_{max} = 141 \text{ KNm}$ $M_n = 139.7 \text{ KNm}$	OK*
$F_{max3} > 0.75 F_{max1}$	$F_{max1} (100\text{kN}; 93\text{kN})$ $F_{max3} (82\text{kN}; 80\text{kN})$	OK OK
$\beta > 0.125$	DE (3880 Nm) IDE (28583 Nm)	OK
$K_{s(\theta=0.035)} > 0.05$	$K_{s(\theta=0.001)} (3.05; 2.35)$	OK
$K_{s(\theta=0.001)}$	$K_{s(\theta=0.035)} (0.86; 0.68)$	OK

* $\lambda = 1.3$, according to [6]

TABLE V
MODEL N2D

Criterion	Values	Conclusions
$E_{max} > E_n$	$M_{max} = 123 \text{ kNm}$ $M_n = 142.8 \text{ kNm}$	Not OK
$E_{max} < \lambda E_n$	$M_{max} = 123 \text{ kNm}$ $M_n = 153.5 \text{ kNm}$	OK*
$F_{max3} > 0.75 F_{max1}$	$F_{max1} (75\text{kN}; 97\text{kN})$ $F_{max3} (75\text{kN}; 93\text{kN})$	OK OK
$\beta > 0.125$	DE (1629 Nm) IDE (13570 Nm)	Not OK
$K_{s(\theta=0.035)} > 0.05$	$K_{s(\theta=0.001)} (1.73; 1.79)$	OK
$K_{s(\theta=0.001)}$	$K_{s(\theta=0.035)} (0.86; 0.68)$	OK

* $\lambda = 1.3$, according to [6]

V. FINAL REMARKS

Despite of the simplicity of the repair technique, taking into account the extreme loading which model was subjected to, up to a drift ratio exceeding 0.06, the second time repaired model N2d does not fulfill all the acceptance criteria, due to the damages of the concrete in the column located in the connection zone and of the grout, beside the failure of the special reinforcement, as can be seen in Fig. 11.

The experimental program is to be continued focused on materials for column-beam interfaces having higher performance, as cementitious advanced materials and on new detailing of the beam ends and column connection zone.

Another direction for widening the research domain is the study of spatial behavior of bidirectional prestressed assembled models having modified hybrid joints.

ACKNOWLEDGMENT

Partial funding for this research was provided by the Executive Agency for Higher Education, Research, Development and Innovation Funding (UEFISCDI), Romania, under grant PN II PCCA 55/2012 “Structural conception and Collapse control performance based DDesign of multistory structures under aAccidental actions” CODEC (2012-2016),

made in the frame of the Partnerships Program Joint Applied Research Projects.

REFERENCES

- [1] Priestley M. J. N., Calvi G. M., Kowalsky M. J., “Displacement Based Seismic Design of Structures”, IUSS Press, Pavia, Italy, 2007.
- [2] ACI Innovation Task Group 1 and Collaborators, “Special Hybrid Moment Frames Composed of Discretely Jointed Precast and Post-Tensioned Concrete Members” (ACI T.1.2-03) and Commentary (ACI T.1.2R-03), American Concrete Institute, USA, 2010.
- [3] Pastrav M. I., Enyedi C., “Hybrid Moment Frame Joints Subjected to Seismic Type Loading”, in *Proceedings of 15th World Conference on Earthquake Engineering*, Lisbon, paper 1343, 2012.
- [4] J Pastrav M., “Sustainable Structures. Seismic Type Loading Behavior of Repaired Reinforced Concrete Hybrid Joint”, in *13th SGEM GeoConference on Nano, Bio and Green – Technologies for a Sustainable Future*, 2013, pp. 465 – 472.
- [5] Pastrav M.I., “Robustness of Modified Special Hybrid RC Frames”, in *11th International Conference on New Trends in Statics and Dynamics of Buildings*, Bratislava, Slovakia, 2013, pp. 175-178.
- [6] Romanian Development, Public Works and Dwelling Minister, “Seismic Design Code - Part I: Building Design Provision” (P100-1), (*in Romanian*), Bucharest, Romania, 2006.
- [7] ACI Innovation Task Group 1 and Collaborators, “Acceptance Criteria for Moment Frames Based on Structural Testing (ACI T1.1-01) and Commentary (ACI T1.1R-01), American Concrete Institute, USA, 2004.